

**OPTICAL TELESCOPE ASSEMBLY
DEFINITION AND REQUIREMENTS
DOCUMENT**

for the

Supernova / Acceleration Probe (SNAP)

**University of California, Berkeley
Lawrence Berkeley National Laboratory**

September 5, 2000

Draft 0.1

1) Background Information

Recent measurements carried out by the Supernova Cosmology Project (SCP) (<http://www-supernova.lbl.gov>) have made the startling discovery that the expansion rate of the universe is accelerating. Physical law requires that some mechanism must drive this expansion rate either through a new form of energy, a new vacuum energy density (cosmological constant), or a yet unknown property of gravity fundamental to the creation and formation of the universe. The source of this acceleration is more powerful than the gravitation from all seen and unseen forms of matter and known energy. The SNAP mission (<http://snap.lbl.gov>) is expected to provide an understanding of the mechanism driving the acceleration of the universe. The satellite observatory is capable of measuring up to 2000 distant type Ia supernovae each year of the three-year mission lifetime. These measurements will map out in detail the expansion rate of the universe at epochs varying from the present to 10 billion years in the past. This is a fundamental test of the theory of inflation (the theory that describes the formation of the universe), and a direct measurement of the key cosmological parameters Ω_m and Ω_Λ . The “accelerating universe” has sparked significant current popular and theoretical interest and several excellent articles can be found in Science, Nature, and Scientific American (<http://snap.lbl.gov/news.html>).

The SNAP observatory will have a 2.0 meter diameter rigid lightweight primary mirror with low obscuration, and a focal plane covering one square degree with diffraction-limited images at 1 micron wavelength. The optical imager will have nearly one billion CCD pixels, representing the largest imager ever fabricated. SNAP is expected to be launched from a Delta III or IV-M rocket. In order to facilitate thermal management of the observatory and instruments, reduce light emissions from the earth’s limb, and minimize the cosmic ray fluence, the spacecraft is placed in high earth orbit above the radiation belts. An artist’s conception of the spacecraft is shown in Figure 1.

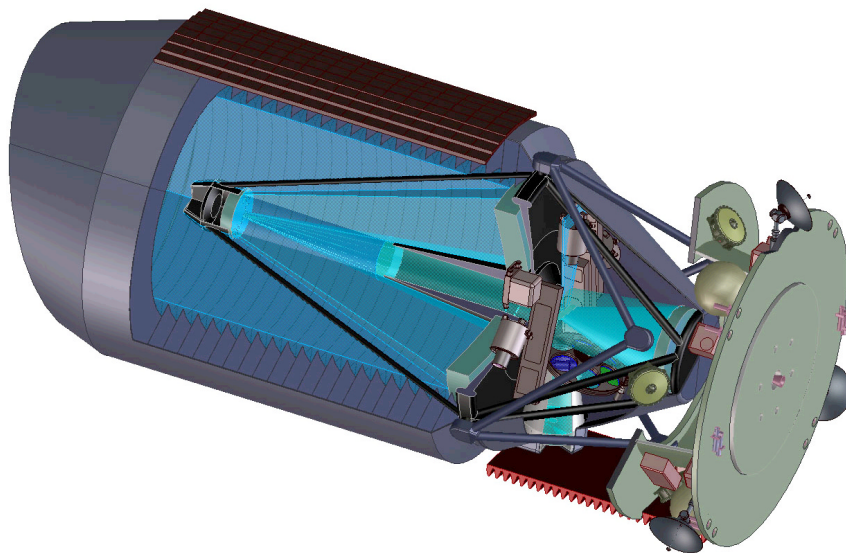


Figure 1. A cutaway of the SNAP satellite is shown in the figure above. The secondary mirror is shown at left while the spacecraft bus and instruments are to the right.

2) Optics Baseline

i. Requirements

There are two key requirements that have driven the concept for the SNAP optical telescope. The first key requirement is the very large – one square degree – field of view. SNAP will carry GigaCAM, a billion pixel camera that will fill this large field of view. This camera is dramatically larger than the Hubble or NGST fields of view as shown in Figure 2. The second key driver is the dimensions of a payload that can be launched in the 4 meter fairing of the Delta III rocket. The nominal 2.0 meter telescope aperture is near the minimum optic size that will allow our science goals to be met, and is near the maximum that can be accommodated within limitations imposed by payload mass and cost. A second driver for our optical design is the requirement for a field of view that supplies a high quality image whose sky area is at least one degree square. Another crucial requirement is a broad bandpass, extending from the near ultraviolet into the near infrared, with no significant chromatic aberration or defocusing.

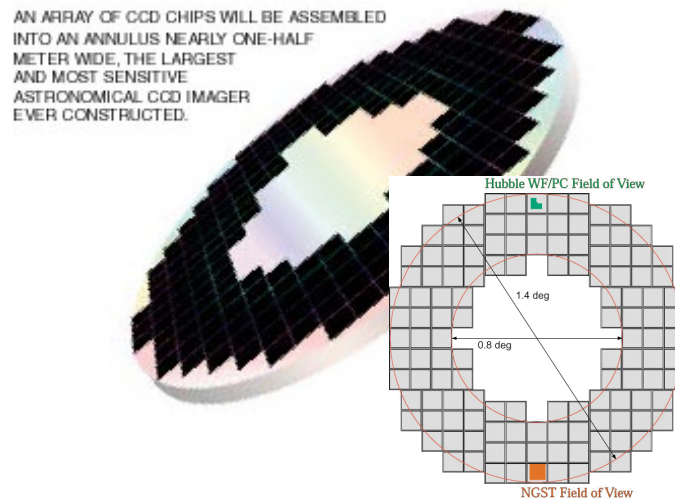


Figure 2. The $1^\circ \times 1^\circ$ imager focal plane populated with 128 $3k \times 3k$, $10.5 \mu m^2$ CCD's.

Since the main detector array will require a mechanical shutter to provide a dark readout environment, and our multiband photometry imposes the need for a multiposition filter wheel in the optical train, the optics must offer a reasonably small beam waist optically conjugate to the entrance pupil where this shutter and a filter wheel can be situated. It is desirable that the optical train avoid the use of refractive lenses or correctors, owing to their susceptibility to cumulative radiation damage on an extreme high altitude orbit such as ours, and due to the production of scintillation and Cerenkov light under charged particle bombardment. Thermally, it is highly advantageous to locate the focal plane at

the cold side of the payload, where radiative detector cooling is straightforward, thereby avoiding the need for heat pipes or refrigerators.

ii. Three mirror anastigmat

The optics design for the SNAP satellite is a variant of a three-mirror telescope explored by M. Paul (M.Paul, Rev.Optics 14 p.169 1935; P.Robb Appl.Opt.17 p.2677 1978). The chief idea is to combine a concave primary paraboloid and a convex secondary paraboloid to approximate an afocal reducer. Followed by a highly concave spherical tertiary. The secondary, located at the center of curvature of the tertiary, is then modified to eliminate the spherical aberration of the tertiary. A 1.8 meter telescope of this type with a 1° field-of-view and a worst case 0.1 arcsec rms radius image was described in 1982 (R. Angel, Woolf & H. Epps, SPIE 332, p.134 1982; also J. McGraw, et al SPIE 331 p.137, 1982). In this design, the short focus of the tertiary places the detector buried deep within the secondary-tertiary space, being inaccessible and blocking its own light and also needs a fairly large secondary 40% of primary size. Placing the tertiary significantly behind the primary was shown by Willstrop in 1984 to have significant advantages for wide-field imaging (Willstrop, R.V., MNRAS 210, 597-609, 1984).

iii. Baseline configuration

Our baseline configuration is a three-mirror anastigmat in which the tertiary mirror re-images an intermediate cassegrain focus onto the detector plane. This configuration has been analyzed by Cook (Cook, L. G. 1979, Proc. Soc. Photo-Opt. Instrum. Eng., 183, 207); Williams (Williams, S. G. 1979, Proc. Soc. Photo-Opt. Instrum. Eng., 183, 212), and is the fifth design presented by Korsch (Korsch, D. 1980, Appl.Opt., 19, 3640). This optical train achieves a large at focal surface with acceptable image quality without the use of refractive correctors. In this design, a concave primary ellipsoid is followed by a convex secondary hyperboloid and a concave tertiary ellipsoid. As with other anastigmats, it is free from spherical aberration, coma and astigmatism. There are further practical advantages to this configuration: baffling against stray light is simpler and the focal plane is more accessible. It possesses two beam waists: one at the cassegrain focus near the primary mirror, and a second midway between the tertiary mirror and the detector plane. This second waist is small, and is an effective location for our filter wheel and CCD shutter. In addition to the three powered mirrors of the TMA, one or more additional at mirrors are essential to repackage the optical train in such a way as to keep the detector assembly from blocking its own light, and make the payload more compact. The folding mirror(s) can be introduced in the space between the secondary and tertiary, and/or the space between the tertiary and the detector. The choice of folding mirror location and angle determines the overall dimensions of the finished payload package.

Our baseline layout is shown in Figure 3. The primary and secondary mirrors are located on the principal axis, as they would be for a conventional cassegrain telescope. The tertiary mirror is on this same axis, far behind the hole in the center of the primary. Immediately behind the primary, a 45 degree at folding mirror extracts the light from the tertiary and directs it to one side, where it comes to a focus on the planar detector array. This final beam segment has a narrow waist and we have located the folding mirror at this

waist to minimize its obscuration of the central part of the field. We utilize the narrow portion of the beam between the folding mirror and the detector to locate the filter wheel assembly and the CCD array shutter. Having the detector located at the cold (shaded) side of the spacecraft permits straightforward passive cooling of the entire CCD array. Our optical arrangement also allows us to generate a secondary optical path for the NIR imager by picking-off light from the backside of the 45 degree folding flat and sending this light to a tertiary mirror.

TMA55 Elevation View

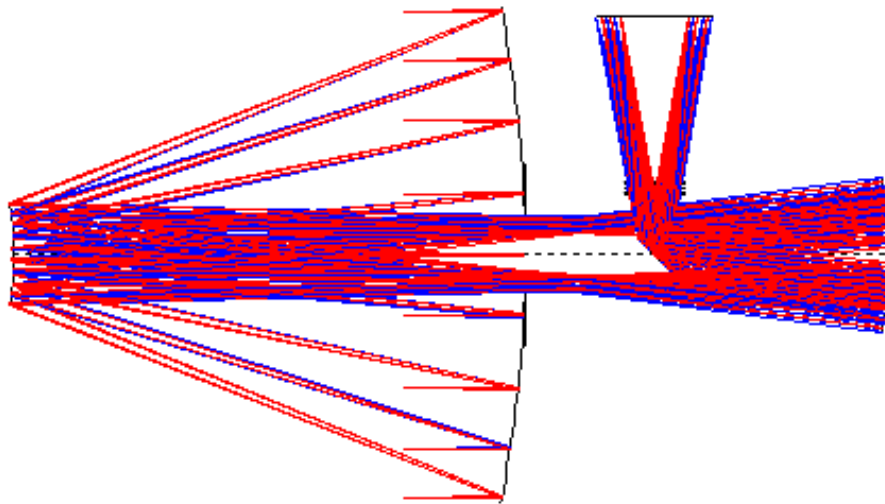


Figure 3. Ray tracing of SNAP three mirror anastigmat design. The annular detector array is shown at top.

We have sized a TMA in this configuration to give a 2.0 meter entrance aperture and a 20 meter focal length, for a plate scale of 100 microns/arcsecond. We have optimized the element curvatures and conic profile shapes to yield the best possible image quality over a one degree diameter field of view. The optical element descriptions for this implementation are given in Table 1.

Table 1. Optical prescription for the SNAP primary optics.

Element	Type	Diameter[m]	Location[m]	Radius Curv.[m]	Shape	Asphericity
Primary Mirror	concave prolate ellipsoid	2.0m, 0.33m hole	0, 0, 0	5.142816	+0.02394	0.976061
Secondary Mirror	convex hyperboloid	0.424	0, 0, -2.1	1.180316	-1.02479	-2.02479
Tertiary Mirror	concave prolate ellipsoid	0.642	0, 0, 1.5	1.52831	+0.44364	-0.55636
Folding Flat Mirror	Oval Flat	0.120x0.192	0, 0, 0.53			
Triple Filter Stack	~5mm thick fused silica	0.25	0.25, 0, 0.53			
Annular Detector		0.278 inner, 0.480 outer	0.98, 0, 0.53			

In Figure 4 is shown the mechanical layout for the SNAP optical prescription. All three powered mirrors are shown as well as the folding flat, the primary focal plane, and the central baffle. In this image the central baffle does not obscure light coming from the primary mirror; however, future stray light analysis will likely require increasing the length of this structure.

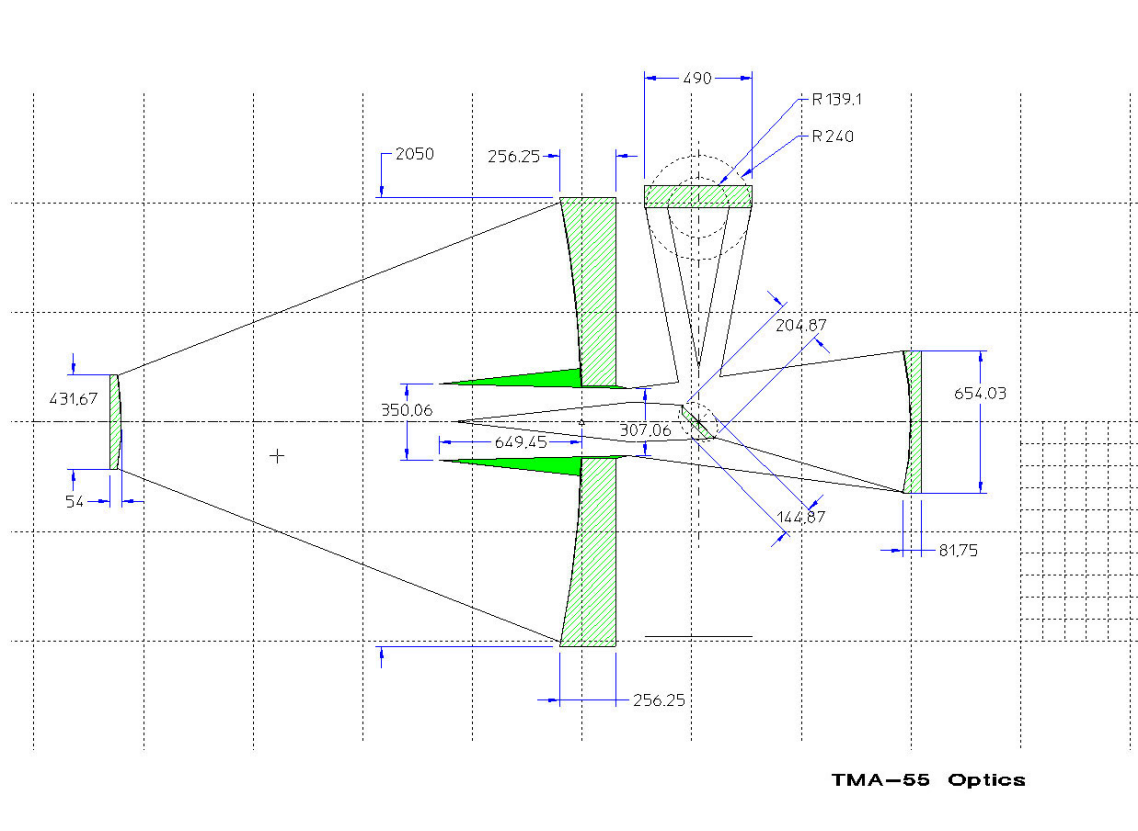


Figure 4. The SNAP optics mechanical layout.

This optic delivers a root-mean-square image blur of 3 microns over a working field of view extending out to 1.0 degrees from the geometrical axis. The folding mirror selects an annular portion of this circular geometrical field for relaying on to the tertiary mirror. This annulus has an inner radius of 0.4 degrees and an outer radius of 0.7 degrees measured on the sky, and is essentially completely unvignetted. The sky area of this subset of image points amounts to 1.0 square degrees, meeting our current requirements. As with all TMA's, the central zone of the field, while having excellent mathematical image quality, is blocked by the folding arrangement needed to extract the tertiary's beam from the secondary's beam. Consequently we do not use the central part of the field for our wide-field imager. This light is however accessible to other instruments placed behind the aperture in the folding mirror. A layout of the instrument bay is shown in Figure 5.

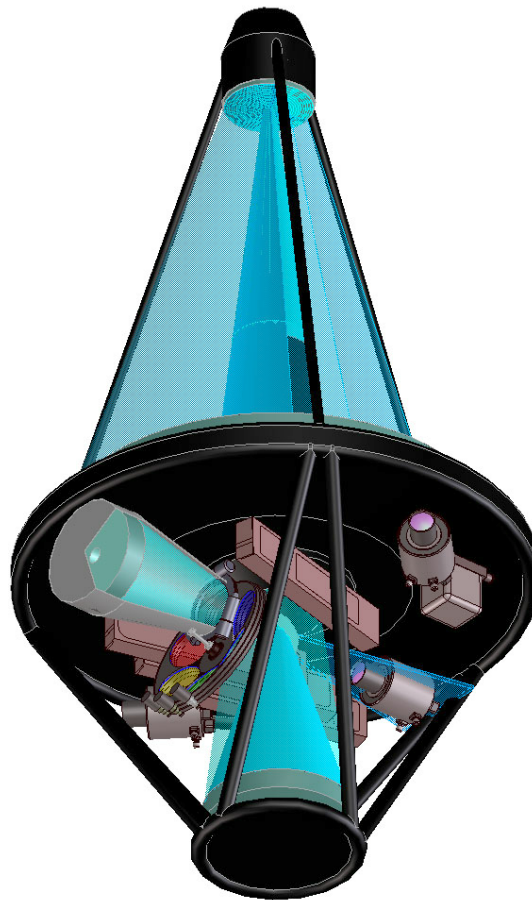


Figure 5. Conceptual satellite optics design for a three mirror anastigmat telescope showing the instrument bay and the tertiary mirror at the bottom. The light path is shown in blue. In this image the filter wheel is visible as well as the large CCD imager at the focal plane.

iv. Filter wheel

The location of the filter wheel is beyond the waist of the beam as shown in Figure 6. At this location the filters will be large and would not normally be parfocal over the full wavelength range of the optical imager. Consequently the filters will have to be manufactured to be parfocal. The filter complement carried will be the standard U, V, B, R, I, Z, plus ten special purpose filters, neutral density filters, and a pass-through.

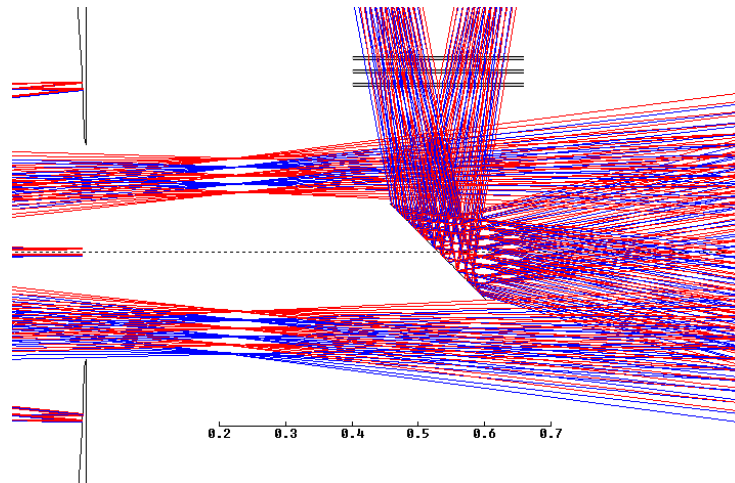


Figure 6. Location of the triple stack of filter wheels.

v. Secondary optics path

Our optical arrangement also allows us to place small additional 45 degree pickoff mirrors in the cassegrain quasifocus plane to feed the NIR imager and other instruments. There may be one or more of these secondary optical paths. They will inhabit the space just behind the primary mirror, immediately ahead of the wide-field imager's 45 degree mirror. There are a number of available auxiliary beam pickoff directions, all generally downward in the Figure 7 below, but clocked at various azimuths around the primary axis.

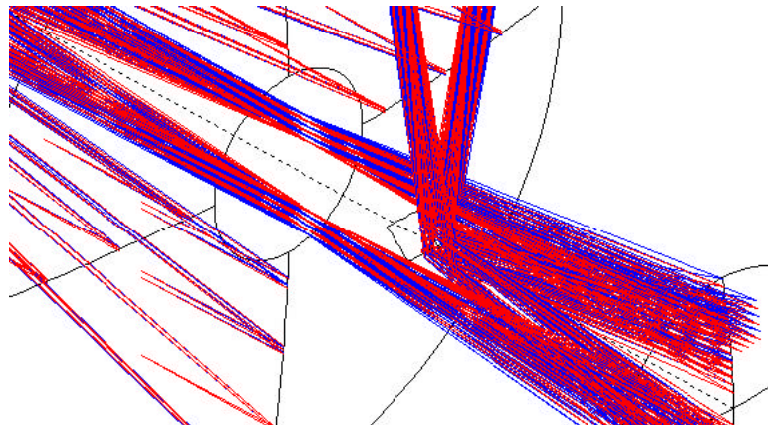


Figure 7. Location of pick-off to generate the secondary optical paths.

The closeup oblique view below shows the space around the Cassegrain focus where these auxiliary optics can be accommodated.

The fields of view and focal lengths for the secondary optical path are still under review. At present we expect the NIR imager to have pixels 18 μ m in size and a plate scale of 0.1 arcsec per pixel, or approximately $f/18$.

Our approach is to provide one or more auxiliary beams from the central part of the cassegrain focus where the primary uncorrected TMA aberration is spherical. This may be easy to correct with a single asphere relay mirror working very slightly off axis. The simplest such configuration is shown below, where a 46 degree pickoff mirror feeds a small concave mirror at the bottom of the figure. This second mirror contains a slight toric correction to compensate for the off normal relay path astigmatism. In layouts such as this, there is only a limited range over which the cassegrain image can be magnified, the limits being due to the available path lengths for the incident and outgoing optical paths to/from the relay. An additional design freedom is the choice of clocking angle about the primary axis, which can be used to locate the final sensor wherever it can be accommodated.

With additional mirrors, a far greater range of possible magnifications becomes practical. One of many such arrangements is shown in Figure 8 below. The pickoff feeds a correcting system of one or more mirrors oriented laterally.

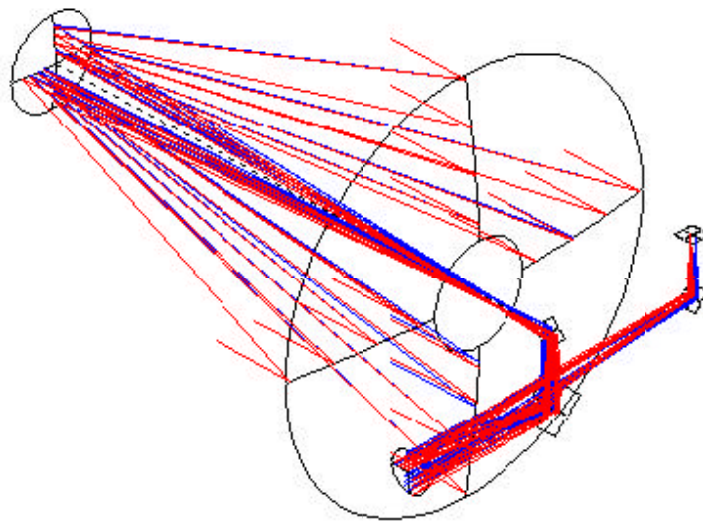


Figure 8. Optical path of the secondary optics path. At bottom left is a small toric mirror used to generated the corrected optical path for the NIR imager shown to the right.

vi. Error budget

The SNAP telescope requires diffraction limited optics at 1 micron wavelength. In order to understand this requirement more fully we briefly look at the derivation of this requirement. The SNAP mission is to examine distant high redshift supernova with an efficiency and performance not obtainable from ground based instruments. The emissions from these supernova are redshifted into the far red and infrared wavelengths. For wavelengths from the U-band to the R-band observing times are short and the operational performance is driven by largely by telemetry. For wavelengths longer than R-band, ie I-band and beyond, the performance of all of the instruments will depend critically on the throughput, and Strehl ratio of the optical system. Strehl Ratio is defined at the "ratio of the intensity at the peak of the aberrated diffraction pattern to the peak of an aberration-free image" in the CodeV reference manual. Observing times in the baseline SNAP mission requirements definition assume a minimum level of performance for these long wavelengths. In Table 2 below we have defined the performance of the telescope at the central wavelength of the I-band with a Strehl ratio of 0.9.

Table 2. SNAP Telescope Optical Error Budget.

SNAP Telescope Optical Error Budget		2 meter	
		Image Diameter (FWHM) arcsec	
Diffraction	Lambda= 830 nm (center of I-band)		0.203
Telescope			
	Primary Mirror		0.075
	Figuring	0.06	
	Thermal Distortion	0.04	
	Support	0.02	
	Alignment	0.01	
	Secondary Mirror		0.026
	Figuring	0.02	
	Thermal Distortion	0.01	
	Support	0.01	
	Alignment	0.01	
	Tertiary Mirror		0.026
	Figuring	0.02	
	Thermal Distortion	0.01	
	Support	0.01	
	Alignment	0.01	
	Misalignment		0.048
	Tracking (sigma=0.02)	0.047	
	Defocus	0.01	
	OVERALL ERROR		0.225

v. Manufacturing tolerances

Manufacturing tolerances for the SNAP optics have been computed and are shown in Table 3 below. In these calculations it has been assumed that all three mirrors are manufactured as a set to the required specification and would generally achieve a Strehl ratio of 0.9 or better. To compensate for variations in the mirror it is assumed that there is full freedom in motion to the mirror separations: primary to secondary, secondary to tertiary, and tertiary to focus. These tolerances apply if the mirrors are made independently. These tolerances are computed with the goal that the worst combination of errors would still give diffraction limited performance at 1 micron: Strehl ratio higher than 0.8. In most combinations of errors, the Strehl exceeds 0.9. In practice, there will not be complete freedom in the locating of all components, and some combinations will result in vignetting by the folding mirror. If all mirrors are at the limits of the tolerances given for both radius and conic constant then the Strehl ratio will be 0.8. Hopefully the probability of this combination is low.

Table 3. Manufacturing tolerances for the SNAP primary optics.

Element	Radius[m]	Conic Constant (Shape-1)
Primary Mirror	5.142816 +/- 0.5%	(+0.02394-1) +/- 0.02%
Secondary Mirror	1.180316 + 0.2% - 0.1%	(-1.02479-1) +/- 0.2%
Tertiary Mirror	1.52831 +/- 0.2%	(+0.44364-1)+/- 0.1%

These tolerances in Table 3 can be relaxed if the primary and secondary mirrors are made first and their radius of curvature and conic constant measured then used to reoptimize the tertiary mirror and the locations of the secondary and tertiary mirrors and of the detector.

In Table 4, the relaxation of the manufacturing tolerances of the primary and secondary mirrors is major. The conic constant, K, is relaxed by a factor of 10 for the primary mirror, and by a factor of 5 for the secondary mirror. The tolerance on radius of curvature of the primary mirror is relaxed by a factor of 2, and by a factor of 5 for the secondary mirror. In this case the clear diameters of the secondary and tertiary must increase slightly to fit any increases of the diameter of illumination caused if the mirrors are moved from their nominal locations in the compensation process.

The radius of curvature, R, and conic constant of the tertiary mirror will not be specified until after the primary and secondary mirrors are made and the as-built R and K measured. In Table 4 the nominal R and K of the tertiary mirror are given followed first by the +/- percentage change that might be required to compensate for errors in the primary and secondary mirrors. The second +/- percent following the tertiary spec is the allowed manufacturing error.

Table 4. Manufacturing tolerances for the SNAP primary optics assuming that the tertiary mirror is manufactured after measuring the primary and secondary mirrors.

Element	Radius[m]	Conic Constant (Shape-1)
Primary Mirror	5.142816 +/- 1.0%	(+0.02394-1) +/- 0.2%
Secondary Mirror	1.180316 + 1.0%	(-1.02479-1) +/- 1.0%

Tertiary Mirror	1.52831 +/- 3.0%	+/- 0.2%	(+0.44364-1)+/- 3%+/-0.1%
-----------------	------------------	----------	---------------------------

The maximum change in magnification (Effective Focal Length) caused by compensation is in the range +6.8% to -6.1%; the location of secondary mirror ranges +/- 38 mm; the location of the tertiary mirror range is +/- 144 mm; the location of the detector ranges +132 -118 mm. It is still being evaluated whether these ranges of motion are permissible within the context of the spacecraft design and the optical bench design. Also, a significant change in the effective focal length could require redesign of the optical imager or loss of field-of-view. The tolerances given should be viewed as the largest permissible given the current knowledge of the SNAP conceptual design.

Manufacturing the tertiary last has a significant benefit on the delivered performance of the optical system. The worst residual Strehl ratio at the wavelength $\lambda = 1000$ nanometers is 0.945, which reduces (worsens) to 0.869 at $\lambda = 632.8$ nm (because the Airy disc is naturally smaller at that wavelength (the geometric spot size does not change in an all-reflecting system)). If the tertiary mirror had an R manufacturing error of 0.1% (instead of +/- 0.2% in Table 4) the worst Strehl ratio would be 0.957 at 1000 nm and 0.896 at 632.8 nm.

The manufacturing errors given in Table 4 for the primary and secondary are not strict limits. They could be larger without significantly reducing the sharpness of the images because the system is compensated. A consequence of a larger error might be a larger change in the magnification (thus of the Effective Focal Length), or larger changes in the locations of the mirrors, on the other hand, larger errors might result in smaller changes required for compensation. It depends on the signs of the errors. (It is complicated but if both the R and K errors are positive for the primary mirror, the change in EFL is also positive.)

Thus, if an excellent conic primary or secondary mirror is made but it is found that its R and/or K are outside the limits in Table 5, the consequence of changing the compensators should be evaluated before more work is done on the mirror.

To achieve a Strehl ratio of 0.9 at the central I-band wavelength (830 nm) the manufacturing wavefront error is likely to require a surface smoothness of $\lambda/8$ at 632.8 micron wavelength. This requirement is still under review.

vi. Mirror weight

Because payload launch costs scale with payload mass, it is an important mission cost minimization tradeoff to reduce payload mass to the point where total cost is least. For this reason we have explored current means for manufacturing lightweight optics and optical support structures. Traditional optical element fabrication methods use solid glass blanks that are rough ground, precision ground, and then polished to give the final optical surface profile and finish. The thickness of each element is chosen to be sufficient to guarantee the stability of the surface figure under stress levels ranging from one gravity

(for figuring and metrology) to zero gravity (use on orbit). Newer lightweight elements use innovative fabrication steps to avoid the mass of solid glass components.

The starting point for low mass optics is the removal from the backside of 60% to 80% of the mass of a solid glass mirror blank. The starting point is a solid disk of Schott Zerodur or Corning ULE glass whose dimensions are close to the desired final dimensions of the mirror. Using abrasive water-jet machining technology, the blank is cut through with numerous hexagonal holes that leave only a thin hexagonal web of glass. Then, a thin solid face sheet and bottom sheet of glass is frit-bonded or fusion-bonded to this honeycomb core. The sandwich is then ground, figured, and polished using advanced low-stress methods such as ion beam milling. The final mirror is typically 60-95% mass relieved since it is mostly empty space. Its rigidity is determined by the box section stiffness of the core glass component with face sheets. This technology is regarded as proven, since it has become a standard military space-surveillance technique, but can be expensive unless the fixturing and bond-bake cycles have been thoroughly explored.

At present, for the SNAP project with a two meter aperture, this technology appears to be our best alternative within fixed cost and schedule constraints. This technique was used on Hubble with a weight relief of 80% and other low altitude missions with good results. This approach is regarded as low risk, and should be able to achieve the mass reduction appropriate for the SNAP mission. The Delta III or Delta IV launch vehicle is capable of lifting approximately 2700 Kg to the proposed orbit. Using this technology mirror weights can be approximated with some simple assumptions as shown in Table 5.

Table 5. Mirror weight (in kg).

Mirror	ULE	rho=	2210		
PMA	2.0 meter		0.5 cassegrain	diameter/thick=	8
	Primary Mirror		325.4	lightweighting=	0.8
SMA	0.42 meter			diameter/thick=	8
	Secondary Mirror		6.4	lightweighting=	0.6
TMA	0.64 meter			diameter/thick=	8
	Tertiary Mirror		22.7	lightweighting=	0.6
TOTAL			354.6		

vii. Optical telescope assembly pointing and rigidity

The pointing accuracy of the SNAP telescope is 0.03 arcsec, mechanical deformations of the OTA should not cause image motion or blur in excess of this amount. The OTA pointing is expected to be actively controlled by a feedback system using a high speed readout from the focal plane to the spacecraft attitude control system. A practical readout speed for the focal plane guider is approximately 30 Hz and would yield a control frequency of approximately 5 Hz. This would mesh well with the capabilities of current spacecraft control systems. This operational assumption divides our requirements into two components: those OTA deformations that are above 5 Hz and those that are below 5

Hz. Above 5 Hz there can be no significant contributions from OTA deformations that cause image motion or defocussing. Below 5 Hz image motion is acceptable since the spacecraft will correct for that; however, deformations that cause defocussing are not permissible.

Allowable motions above 5 Hz are:

Tight tolerances are required for the case of jitter where nothing is moved to compensate. The tolerances of the secondary mirror are especially tight because of the fast focal ratio, of the primary mirror. The decentrations (Δy), piston (Δz) and tilts (x') of the SNAP secondary and tertiary mirrors that produce ± 0.03 arcsec ($2.9 \mu\text{m}$) of image motion or image blur are, with no compensators:

Element	Δy	x'	Δz
Secondary Mirror	$0.5 \mu\text{m}$	$0.4 \mu\text{rad}$	$1.2 \mu\text{m}$
Tertiary Mirror	$1.2 \mu\text{m}$	$0.7 \mu\text{rad}$	$19 \mu\text{m}$

The Δz of $1 \mu\text{m}$ for the secondary and $19 \mu\text{m}$ for the tertiary also can be interpreted as the maximum step intervals in the focusing mechanism.

Allowable motions below 5 Hz are:

If there is a tilt or decentration error in the telescope, what matters is the blur caused by optical aberrations, not displacement of an axial image from the center of the field of view because the telescope can simply be repointed to center the field on the detector. Another important compensator is the tilt of the focal surface (tilt of the detector). The blur is calculated as a $2.9 \mu\text{m}$ increase in separation at the focus of rays that originate on the entrance pupil at one half of the pupil diameter. The following tolerances are for the case where the telescope is perfectly aligned except for the listed alignment error:

Element	Δy	x'
Secondary Mirror	$5.2 \mu\text{m}$	$8.4 \mu\text{rad}$

Each of the above errors produce 0.03 arcsec of coma. The tilt of the secondary mirror also produces a small amount astigmatism.

viii. Optical Coatings

Enhanced Silver on the primary, secondary, and tertiary
 Gold (?) on IR secondary optics path for reduced emissivity in IR

Expected total throughput:

Element	Throughput
---------	------------

Coatings (4 refl.)	>0.92
Secondary Obscuration	0.95
Secondary Truss	0.95
Secondary Baffle	0.98
Central Baffle	0.98
TOTAL THROUGHPUT	>0.80

viii. Thermal Environment

Around 250K for optical surfaces – still under review

ix. OTA Components

Kinematic mounts for primary

Primary Mirror Assembly (PMA)

Optics Bench

Tertiary Mirror Assembly (TMA)

Secondary Mirror Assembly (SMA) 5% obscuration



Figure 9. Secondary Mirror Assembly

x. Summary of Requirements

Element	Requirement	Comment
---------	-------------	---------

Primary mirror diameter	2.0 meter diameter	Cost driven requirement
Secondary mirror diameter	0.42 meter diameter	
Tertiary mirror diameter	0.64 meter diameter	
Primary mirror hole	0.5 meter diameter	
Primary mirror focal ratio	f/1.285	
Optical coating	Enhanced Silver	
Optical surface finish	$\lambda/8$ @ 632.8 nm	
Strehl ratio	0.9 @ 830 nm	
Temperature of optics	250 K	Under study
Obscuration by SMA truss	< 5 %	
Obscuration by baffles	< 10 %	Under study
Primary Mirror Mass	~325 kg	
Secondary Mirror Mass	~7 kg	
Tertiary Mirror Mass	~ 23 kg	
Resonant frequency	> 35 Hz	
Wavelength range	350 nm – 1700 nm	
Throughput	> 90% for $\lambda > 800$ nm	Excludes SMA & baffles

xi. Known issues

- 1) Thermal management, optics temperature
- 2) Clearance of detector from bottom of primary
- 3) Secondary optics path
- 4) Surface smoothness
- 5) Stray light prevention, analysis of baffling